Hubble Space Telescope imaging of the optical emission-line filaments of NGC 1275

March 3, 2008

A.C. Fabian[1], R.M. Johnstone[1], J.S. Sanders[1], C.J. Conselice[2], C.S. Crawford[1], J.S. Gallagher III[3] and E. Zweibel[3,4]

1. Institute of Astronomy, Madingley Road, Cambridge CB3 0HA, UK
2. University of Nottingham, School of Physics & Astronomy, Nottingham NG7 2RD, UK
3. Department of Astronomy, University of Wisconsin, Madison, WI 53706, USA
4. Department of Physics, University of Wisconsin, Madison, WI 53706, USA

The giant elliptical galaxy NGC 1275, at the centre of the Perseus cluster, is surrounded by a well-known nebulosity of emission-line filaments[1][2]. They are embedded in the 40 million K, X-ray emitting, intracluster medium of the cluster core and stretch for over 80 kpc, with an organised velocity field of $100-200\,\mathrm{km\,s^{-1}}$ [3]. This means that they are plausibly about $>10^8$ yr old. It has recently been found that the mass of even the outer filaments is dominated by molecular gas[4][5]. It is likely that they have been dragged out from the centre of the galaxy by the radio bubbles rising buoyantly in the hot intracluster gas[3]. In essence, the filaments are dramatic markers of the feedback process by which energy is transferred from the central massive black hole to the surrounding gas. Here we present images of the filament system taken with the Advanced Camera for Surveys (ACS) of the Hubble Space Telescope (HST) and find fine threadlike structure which is just resolved in the filaments. Some threads extend over 6 kpc yet are only 70 pc wide. We find that magnetic fields in pressure balance with the surrounding hot gas are necessary to maintain the integrity of the filaments against tidal shear.

The images presented here (Figs. 1-4) were taken with the ACS camera on HST using three filters. The broadband red filter, F625W, passes the redshifted Halpha line from both the low and high-velocity emission-line systems as well as red continuum; a medium bandwidth green filter, F550M, samples nearby continuum and is almost completely free from strong emission lines. The broadband blue filter, F435W is sensitive to light from young stars, but also passes some light from the from the [OII]λ3727 emission line.

Multiple exposures using a three-point line dither pattern were taken at a set of three pointing positions around the centre of NGC 1275 in filters F550M and F625W with considerable overlap between the pointings. Similar data were obtained in the F435W filter, but from only two pointing positions because of the failure of ACS before the completion of this programme. The data from each filter were registered relative to each other using stars and then combined separately into large mosaic images using the latest version of the stsdas task multidrizzle[6].

In Fig. 2 we show part of the Northern filament $\sim 27\,\mathrm{kpc}$ from the nucleus (we adopt $H_0 = 71\,\mathrm{km\,s^{-1}\ Mpc^{-1}}$ which at a redshift 0.0176 for NGC 1275 gives 352 pc arcsec^{-1}). The filaments seen in the WIYN ground-based image (right) are just resolved into narrow threads with the HST ACS. This also occurs in many other filaments including the NW 'horseshoe' filament (Fig. 3) which lies

immediately interior to the outer ghost bubble in X-ray images[8]. A fine thread of emission is seen in the Northern filament system extending about 16 arcsec or 5.8 kpc. Averaged over kpc strips it is about 4 pixels (0.2 arcsec) or about 70 pc wide. (This is an upper limit as the PSF of the ASC is about one half this value.) The aspect ratio (length / thickness) therefore approaches 100. The top of the horseshoe which is about 6 kpc across is similar, as are many other relatively isolated filaments. We adopt a radius of 35 pc for modelling the fine threads.

The radial velocity shear along the filaments is about $100 - 200\,\mathrm{km\,s^{-1}}$ [3]. If we assume that after correction for projection the velocity shear is about $300\,\mathrm{km\,s^{-1}}$ then, considering the whole structure out to a radius of 50 kpc, it must be $1 - 2 \times 10^8\,\mathrm{yr}$ old. Individual filaments may be in ballistic motion, falling back in for example, but to retain their structure over this time means that something must balance gravity or at least tidal gravitational forces. For a filament of radial length ℓ at radius r the gravitational acceleration $g \sim v^2/R$, where v is the velocity dispersion in the potential (about $700\,\mathrm{km\,s^{-1}}$ at that radius as inferred from the X-ray measured temperature of the intracluster medium[10]) at radius $R \sim 25$ kpc and tidal acceleration is smaller by $2\ell/R$. The most likely force to balance a filament against gravity is the tangential component of a magnetic field.

In order to estimate the required magnetic field we need to know the properties of a filament and its surroundings. We shall concentrate on a thread of radius 30 pc and length 6 kpc at a distance of 25 kpc from the nucleus of NGC 1275 as a basic structural unit typical of what is now resolved in the filaments. We estimate a total mass for such a thread using the total gas mass of $10^8\,\mathrm{M_\odot}$, inferred from CO emission[7] observed in a 22 arcsec IRAM beam on the Northern filament complex. Assuming that the mass scales with Hα emission, which appears to be the case for the H_2 emission measured with Spitzer[11], then our fiducial thread has a mass of about $10^6\,\mathrm{M_\odot}$. Its mean density is then $\sim 2\,\mathrm{cm^{-3}}$ and perpendicular column density $N \sim 4 \times 10^{20}\,\mathrm{cm^{-2}}$ or $\Sigma_\perp \sim 7 \times 10^{-4}\,\mathrm{g\,cm^{-2}}$. The lengthwise column density is ℓ/r times larger.

Consider first a horizontal thread supported against gravity, the field B_h needed for support is then $B_\mathrm{h} \sim (4\pi\Sigma_\perp g)^{1/2}$. For the above values this corresponds to $B_\mathrm{h} \sim 24\mu$G which is less than the equipartition value of $80\ \mu$G so energetically possible. By equipartition we mean that $B^2/8\pi = nkT$ and use the total particle density $n = 0.06\,\mathrm{cm^{-3}}$ and temperature $T = 4\,\mathrm{keV}$ for the X-ray emitting surrounding gas[10]. For a radial filament the value is $(R/\ell)^{1/2} \sim 40$ times larger which is a problem. We gain some agreement by balancing just the tidal stress. Note that the required magnetic field is inversely proportional to the radius of the filamentary threads which means that the high spatial resolution of the HST is essential for demonstrating the high magnetic field required in the NGC 1275 system.

The filaments are therefore magnetically-dominated (ratio of thermal to magnetic pressure $\beta < 1$) and are essentially magnetic molecular structures, similar (but at much higher surrounding pressures) to Galactic molecular clouds[9][12]. We assume of course that the magnetic field is coupled to the (low) ionized fraction of the cold gas and that the slowness of ambipolar diffusion links the molecular, atomic and ionized components. The emission from the filaments is likely energised by magnetic waves powered by the kinetic energy of the clouds[13]. The observed FWHM velocity dispersion of $\sim 100\,\mathrm{km\,s^{-1}}$ [3] within a filament may be direct evidence of such waves as indeed expected for Alfvenic turbulence, where half the internal pressure is kinetic and half magnetic.

We now turn to the issue of star formation in the filaments. Many massive star clusters were discovered across the face of NGC 1275 in early HST imaging[14][15], most of which do not correlate in position with any filaments. However to the SE and S there are examples of ordered chains of young star clusters (Fig. 4). They are offset from the nearest Hα filaments by a few kpc. The ones to the SE resemble short streamers and are probably unbound clumps falling apart in the tidal cluster field. This gives an age for the clumps of about 20 Myr. Their association with the filaments, particularly the one to the S, shows that stars do sometimes form in the filaments and that at least part of the enormous star cluster system of NGC 1275 originates in this way. In general though there are no obvious star clusters associated with the filaments, so at any given time the star formation rate in any filament must be low.

The critical surface density Σ_c for gravitational instability corresponding to the magnetic field we infer in the filaments is given by $\Sigma_\mathrm{c} = B/2\pi\sqrt{G} = 0.062(B/100\mu G)\,\mathrm{g\,cm^{-2}}$ or a critical column

density of $N_{\rm c} = 4 \times 10^{22}\,{\rm cm}^{-2}$ (assuming hydrogen). Given the mean density of a thread of $\sim 2\,{\rm cm}^{-3}$ and transverse column density $\sim 2 \times 10^{20}\,{\rm cm}^{-2}$, they are gravitationally stable. Instability could occur however, if either much of the molecular mass is concentrated in a much smaller thickness ($\sim 0.1\,{\rm pc}$ for 50 K, assuming thermal pressure balance) and $\beta > 1$, or if the field becomes well ordered parallel to a radial filament axis. Thus gravitational stability depends on the configuration of the molecular and magnetic components.

If a filament acts as a coherent unit due to the magnetic field, then it will interact dynamically with the hot, low density, surrounding gas over a length scale corresponding to its own column density. The above mean value of $2 \times 10^{20}\,{\rm cm}^{-2}$ corresponds to about 1 kpc ($\sim$ 3 arcsec) in the surrounding hot gas, so the relative straightness of many filaments over scales of 3–10 kpc or more shows that motions in that gas must be reasonably ordered and not highly turbulent on those scales[8]. We note that the volume-filling component of a filament is probably the 5 million K, soft X-ray emitting phase seen in Chandra X-ray images[16].

Filamentary emission-line structures are common in massive young galaxies[17]. The filament system of NGC 1275 may be a nearby example which can be observed in unprecedented detail. The outer filaments of NGC 1275 present us with magnetically-dominated molecular clouds stretched out for individual inspection. Here we have shown that many of these filaments are composed of fine threads which are just resolved by HST.

References

[1] Kent S.M., Sargent W.L.W., 1979, ApJ, 230, 667

[2] Conselice C.J., Gallagher III J.S., Wyse R.F.G., 2001, AJ, 122, 2281

[3] Hatch N.A., Crawford C.S., Johnstone R.M., Fabian A.C., 2006, MNRAS, 367, 433

[4] Hatch N.A., Crawford C.S., Fabian A.C., Johnstone R.M., 2005, MNRAS, 358, 765

[5] Salome P. et al, 2007, A&A, 454, 437

[6] Koekemoer, A. M.; Fruchter, A. S.; Hook, R. N.; Hack, W., 2003, Proceedings of The 2002 HST Calibration Workshop, Edited by Santiago Arribas, Anton Koekemoer, and Brad Whitmore. Space Telescope Science Institute, 2002., p.337

[7] Salome P., Combes P., Revaz Y., Edge A.C., Hatch N.A., Fabian A.C., Johnstone R.M., 2008, A&A submitted

[8] Fabian A.C., Sanders J.S., Crawford C.S., Conselice C.J., Gallagher III J.S., Wyse, R.F.G., 2003, MNRAS, 344, L48

[9] Heiles C., Crutcher R., 2005, Lecture Notes in Physics, 664, Springer, Berlin, p137

[10] Fabian A.C., Sandesr J.S., Taylor G.B., Allen S.W., Crawford C.S., Johnstone R.M., Iwasawa K., 2006, MNRAS, 366, 417

[11] Johnstone R.M., Hatch N.A., Ferland G.J., Fabian A.C., Crawford C.S., Wilman R., 2007, MNRAS, 382, 1246

[12] McKee, C. F., Zweibel, E. G., Goodman, A. A., Heiles, C., 1993, Protostars and Planets III, Eds, Eugene H. Levy, Jonathan I. Lunine, University of Arizona Press, Tucson, Arizona, p327

[13] Ferland G.J., Fabian A.C., Hatch N.A., Johnstone R.M., Porter R.L., van Hoof P.A.M., Williams R.J.R., 2008, MNRAS, submitted [arXiv 0802.2535]

[14] Holtzman J.A., et al 1992, AJ. 103. 691

[15] Carlson M.N. et al, 1998, AJ, 115, 1778

[16] Sanders J.S., Fabian A.C., 2007, MNRAS, 381, 1381

[17] Reuland M., et al, 2003, ApJ, 592, 755

[18] Bertin E., Arnouts S., 1996, A&AS, 117, 393

[19] Joye W.A., Mandel E., 2005, ASPC, 347, 110

[20] Lupton R., Blanton M.R., Fekete G., Hogg D.W., O'Mullane W., Szalay A., Wherry N., PASP, 2004, 116, L133

1 Acknowledgements

ACF thanks the Royal Society for support.

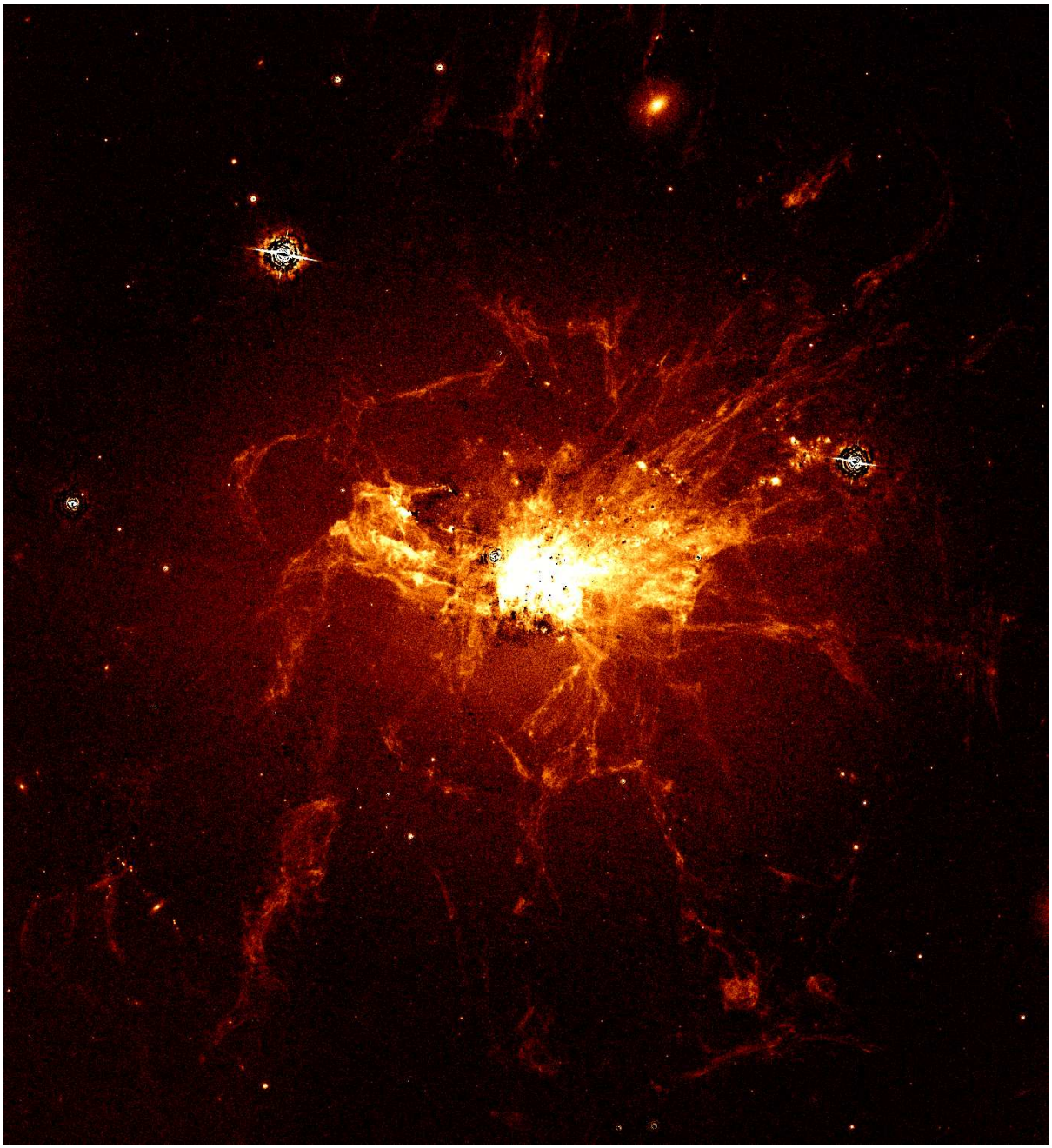

Figure 1: Image of the Hα emission from the core of the cluster. This was created by subtracting a scaled green image from the red image, removing the smooth galactic continuum ontribution. The image measures 140x150 arcsec in size.

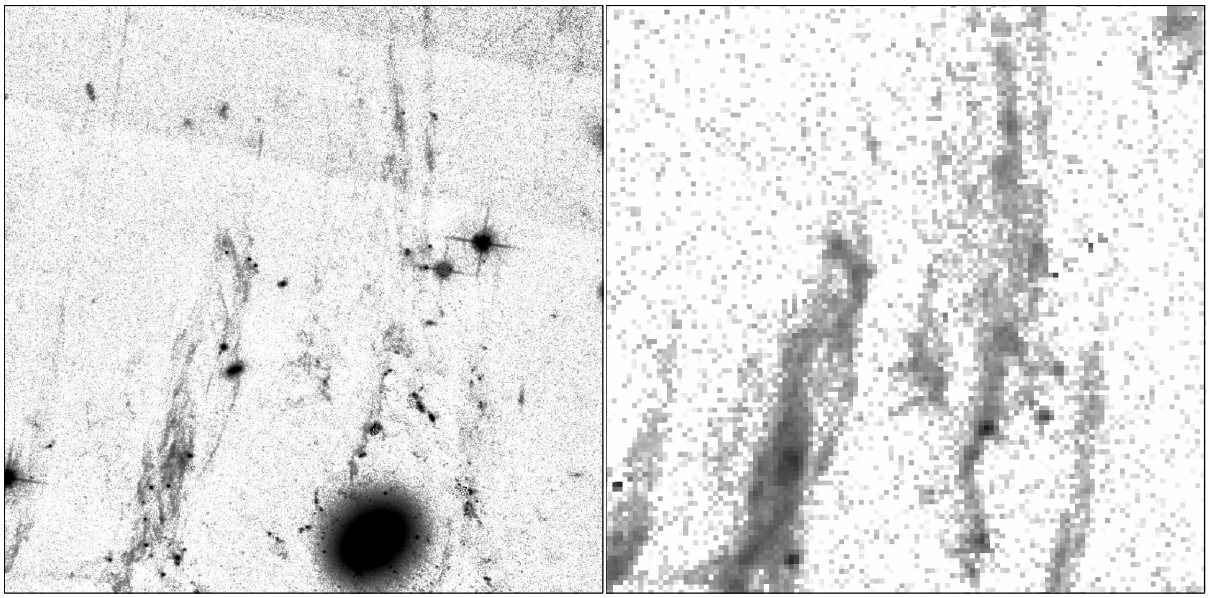

Figure 2: Northern filament system about 25 kpc N or the nucleus from ACS data (left) and WIYN telescope (right; from[2]). The ACS image was produced from the red filter. The SExtractor tool[18] was applied to the data to identify sources and create a model for the smooth galactic light. This was subtracted from the red filter image to enhance the filament. The SExtractor neural network was used to identify stellar sources. These sources were hidden by filling their regions with random values selected from the surrounding pixels. Each image measures 46.6x46.1 arcsec in size.

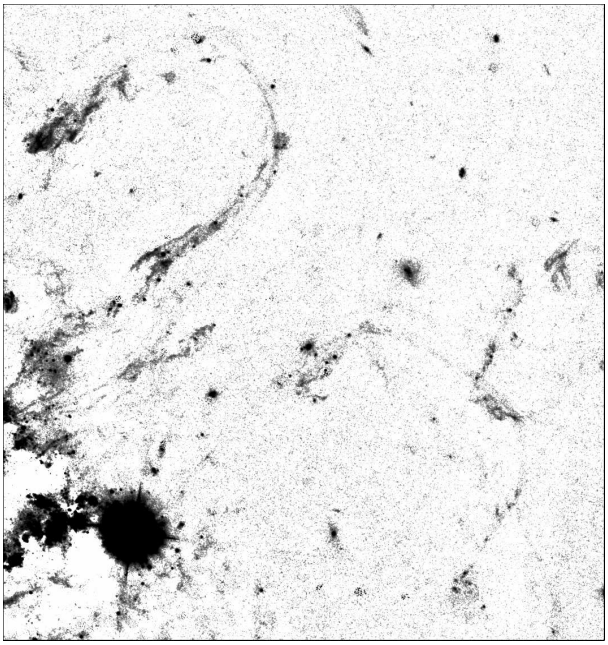

Figure 3: Horseshoe filament system about 25 kpc to the NW of the nucleus. This image has had continuum and stellar sources removed in the same way as Fig 2. The image measures 53.5x56.5 arcsec in size.

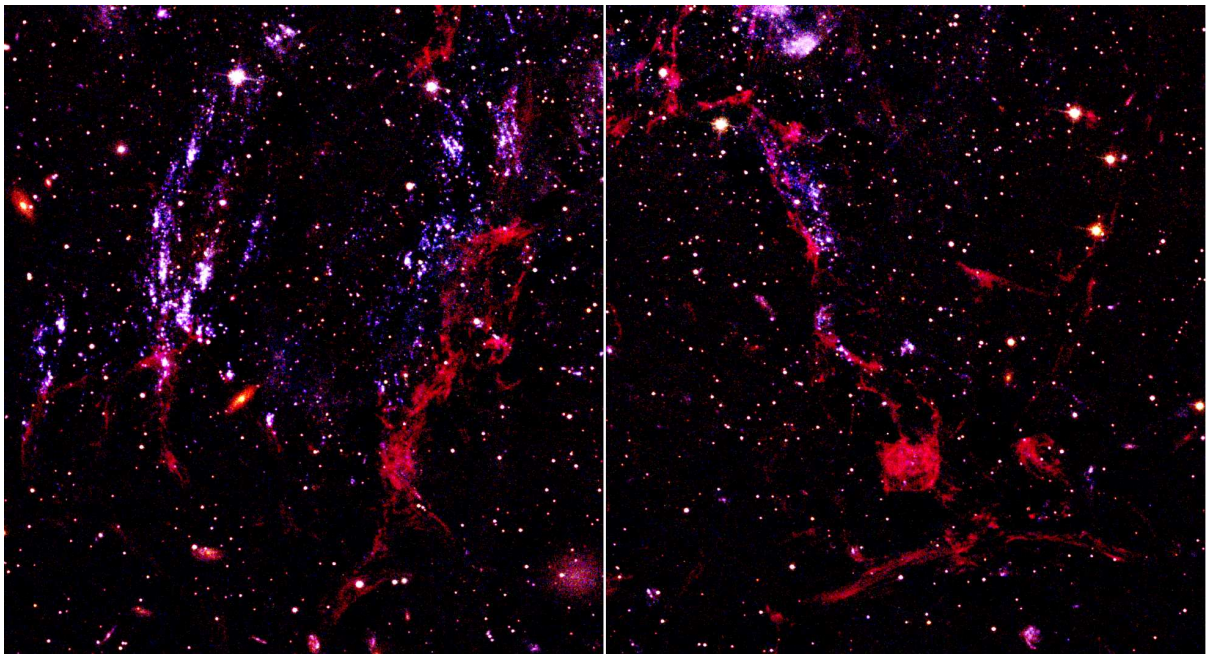

Figure 4: Clumps of stars and Ha filaments seen to the SE and S of the nucleus. SExtractor was used to model the smooth galactic light in the red, green and blue bands. This continuum was subtracted from each image. The images were combined as red, green and blue channels with SAOImage DS9[19].

2 Supplementary text

The full list of observations is given in Table 1.

We show a complete red, green and blue image in Fig. 5 and the Hα emission contrasted with the blue emission (mainly young stars) in Fig. 6. Part of the blue stellar emission to the N of the nucleus is from the High Velocity System (HVS) which is superimposed on NGC 1275, yet must lie 100 kpc or more closer to us [16]. The 'spray' of stars to the N is also likely due to the HVS.

In Fig. 7 the Hα emission is overlaid on a 2–8 keV Chandra X-ray image. This X-ray band emphasises the pressure of the hot intracluster gas and thus shows the weak shocked surrounding the radio bubbles N and S of the centre. It is interesting that the tangential filaments which lie at the ends of several radial filaments (e.g. to the S and W) occur close to this shock.

Closeup images of several features are shown in Fig. 8. To the left is a 'fossil fish'-like structure which straddles the weak shock to the SE. The 'tail' of the 'fish' has fine structure. The S and E tangential filaments shown in the centre and right images consist of several parallel fine structures.

To assess the thickness of the fine threads we have examined cuts through several of them (Fig. 9). The images have been drizzled onto 0.025 arcsec pixels so 40 pixels correspond to one arcsec. The profiles left to right correspond to the boxes left to right with the profile of a typical star overlaid in red. The stellar profile is obviously narrower than any of the filaments.

Table 1: Log of observations

Pointing	RA(2000)	Dec (2000)	Date	Filter	Exposure(s)	p.a.(deg)
NGC1275-SW	3 19 45.3	41 30 40.0	2006-07-29	F435W	815.0	260.3
NGC1275-SW	3 19 45.6	41 30 40.7	2006-07-29	F435W	815.0	260.3
NGC1275-SW	3 19 45.8	41 30 41.5	2006-07-29	F435W	815.0	260.3
NGC1275-SW	3 19 45.3	41 30 40.0	2006-07-30	F435W	824.0	260.3
NGC1275-SW	3 19 45.6	41 30 40.7	2006-07-30	F435W	824.0	260.3
NGC1275-SW	3 19 45.8	41 30 41.5	2006-07-30	F435W	824.0	260.3
NGC1275-SE	3 19 50.5	41 30 40.0	2006-08-04	F435W	815.0	257.9
NGC1275-SE	3 19 50.8	41 30 40.9	2006-08-04	F435W	815.0	257.9
NGC1275-SE	3 19 51.0	41 30 41.7	2006-08-04	F435W	815.0	257.9
NGC1275-SE	3 19 50.5	41 30 40.0	2006-08-05	F435W	824.0	257.9
NGC1275-SE	3 19 50.8	41 30 40.9	2006-08-05	F435W	824.0	257.9
NGC1275-SE	3 19 51.0	41 30 41.7	2006-08-05	F435W	824.0	257.9
NGC1275-NW	3 19 45.3	41 31 60.0	2006-08-08	F550M	806.0	256.4
NGC1275-NW	3 19 45.3	41 31 60.0	2006-08-08	F550M	806.0	256.4
NGC1275-NW	3 19 45.6	41 32 0.9	2006-08-08	F550M	806.0	256.4
NGC1275-NW	3 19 45.6	41 32 0.9	2006-08-08	F550M	806.0	256.4
NGC1275-NW	3 19 45.8	41 32 1.9	2006-08-08	F550M	806.0	256.4
NGC1275-NW	3 19 45.8	41 32 1.9	2006-08-08	F550M	806.0	256.4
NGC1275-SW	3 19 45.3	41 30 40.0	2006-07-29	F550M	806.0	260.3
NGC1275-SW	3 19 45.3	41 30 40.0	2006-07-29	F550M	806.0	260.3
NGC1275-SW	3 19 45.6	41 30 40.7	2006-07-29	F550M	806.0	260.3
NGC1275-SW	3 19 45.6	41 30 40.7	2006-07-29	F550M	806.0	260.3
NGC1275-SW	3 19 45.8	41 30 41.5	2006-07-29	F550M	806.0	260.3
NGC1275-SW	3 19 45.8	41 30 41.5	2006-07-29	F550M	806.0	260.3
NGC1275-SW	3 19 45.3	41 30 40.0	2006-07-29	F550M	813.0	260.3
NGC1275-SW	3 19 45.3	41 30 40.0	2006-07-29	F550M	813.0	260.3
NGC1275-SW	3 19 45.6	41 30 40.7	2006-07-29	F550M	813.0	260.3
NGC1275-SW	3 19 45.6	41 30 40.7	2006-07-29	F550M	813.0	260.3
NGC1275-SW	3 19 45.8	41 30 41.5	2006-07-29	F550M	813.0	260.3
NGC1275-SW	3 19 45.8	41 30 41.5	2006-07-29	F550M	813.0	260.3
NGC1275-SE	3 19 50.5	41 30 40.0	2006-08-04	F550M	806.0	257.9
NGC1275-SE	3 19 50.5	41 30 40.0	2006-08-04	F550M	806.0	257.9
NGC1275-SE	3 19 50.8	41 30 40.9	2006-08-04	F550M	806.0	257.9
NGC1275-SE	3 19 50.8	41 30 40.9	2006-08-04	F550M	806.0	257.9
NGC1275-SE	3 19 51.0	41 30 41.7	2006-08-04	F550M	806.0	257.9
NGC1275-SE	3 19 51.0	41 30 41.7	2006-08-04	F550M	806.0	257.9
NGC1275-SE	3 19 50.5	41 30 40.0	2006-08-04	F550M	813.0	257.9
NGC1275-SE	3 19 50.5	41 30 40.0	2006-08-04	F550M	813.0	257.9
NGC1275-SE	3 19 50.8	41 30 40.9	2006-08-04	F550M	813.0	257.9
NGC1275-SE	3 19 50.8	41 30 40.9	2006-08-04	F550M	813.0	257.9
NGC1275-SE	3 19 51.0	41 30 41.7	2006-08-05	F550M	813.0	257.9
NGC1275-SE	3 19 51.0	41 30 41.7	2006-08-05	F550M	813.0	257.9
NGC1275-NW	3 19 45.3	41 31 60.0	2006-08-08	F625W	827.0	256.4
NGC1275-NW	3 19 45.6	41 32 0.9	2006-08-08	F625W	827.0	256.4
NGC1275-NW	3 19 45.8	41 32 1.9	2006-08-08	F625W	827.0	256.4
NGC1275-SW	3 19 45.3	41 30 40.0	2006-07-29	F625W	827.0	260.3
NGC1275-SW	3 19 45.6	41 30 40.7	2006-07-29	F625W	827.0	260.3
NGC1275-SW	3 19 45.8	41 30 41.5	2006-07-29	F625W	827.0	260.3
NGC1275-SW	3 19 45.3	41 30 40.0	2006-07-29	F625W	827.0	260.3
NGC1275-SW	3 19 45.6	41 30 40.7	2006-07-29	F625W	827.0	260.3
NGC1275-SW	3 19 45.8	41 30 41.5	2006-07-30	F625W	827.0	260.3
NGC1275-SE	3 19 50.5	41 30 40.0	2006-08-04	F625W	827.0	257.9
NGC1275-SE	3 19 50.8	41 30 40.9	2006-08-04	F625W	827.0	257.9
NGC1275-SE	3 19 51.0	41 30 41.7	2006-08-04	F625W	827.0	257.9
NGC1275-SE	3 19 50.5	41 30 40.0	2006-08-05	F625W	827.0	257.9
NGC1275-SE	3 19 50.8	41 30 40.9	2006-08-05	F625W	827.0	257.9
NGC1275-SE	3 19 51.0	41 30 41.7	2006-08-05	F625W	827.0	257.9

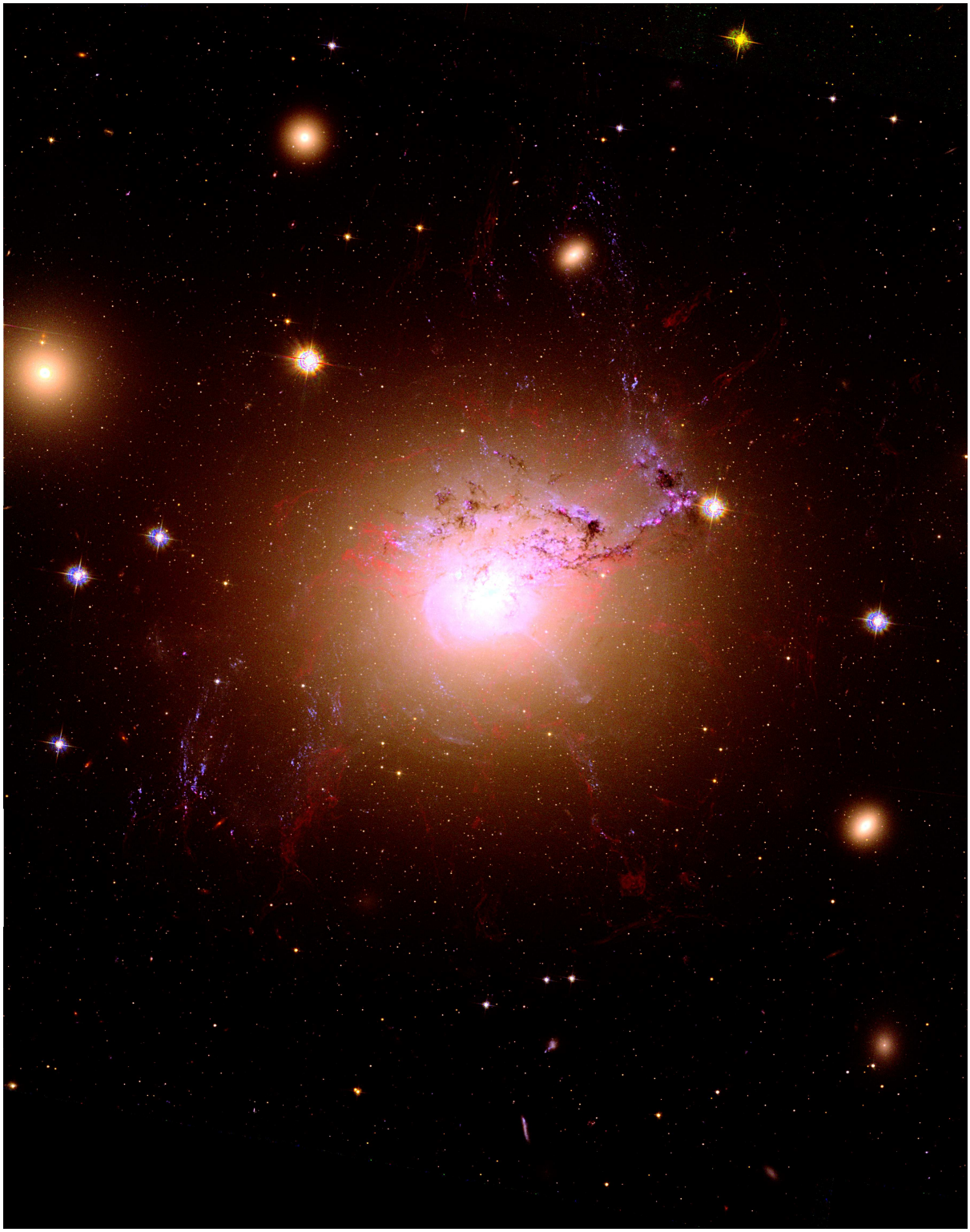

Figure 5: Colour image created by combining the data using the three ACS filters. The three images were processed with the method of [20] to preserve the colour of objects avoiding saturation. The detail in the Hα filaments was enhanced by using the unsharp mask filter in the GNU Image Manipulation Tool.

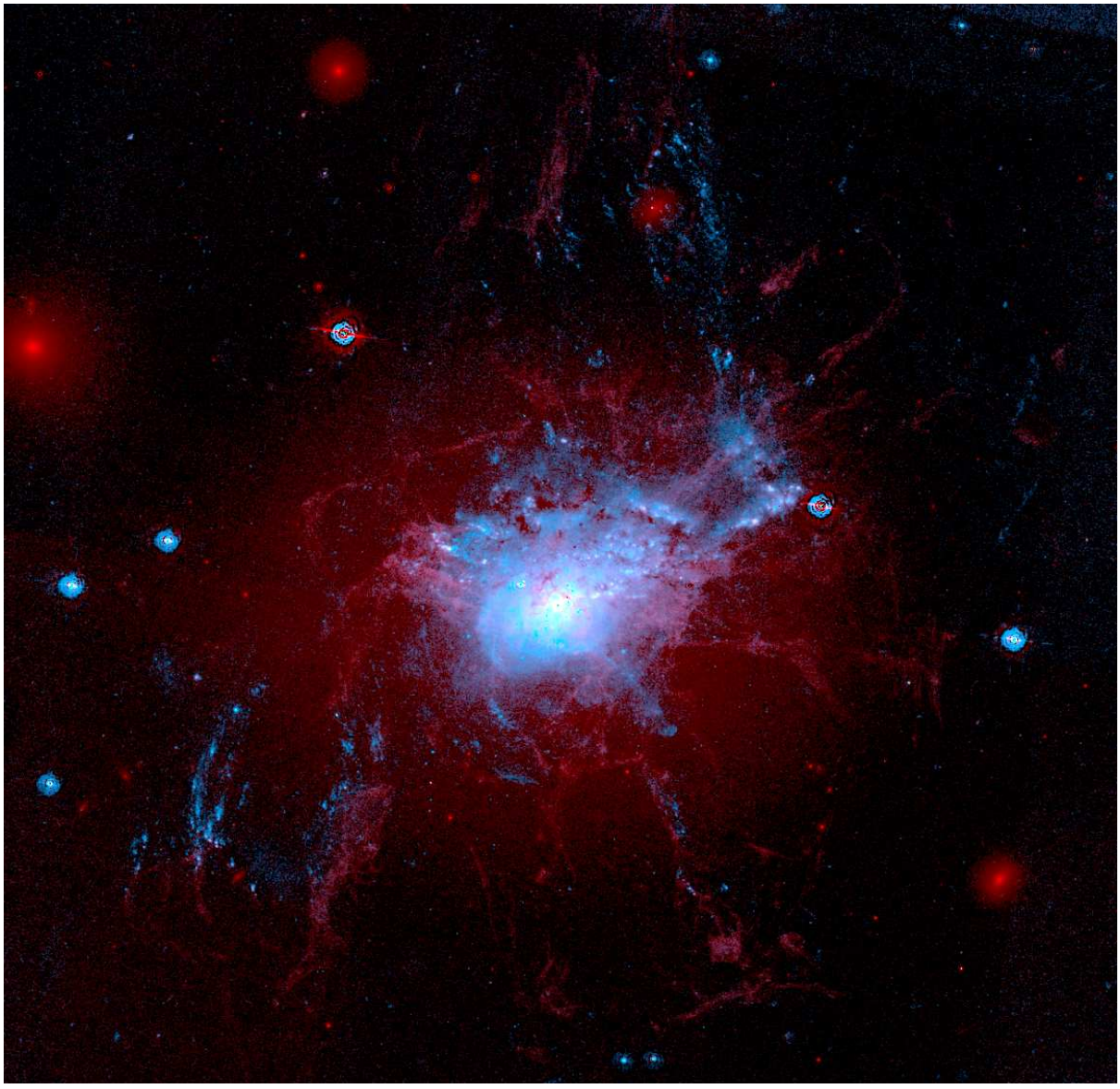

Figure 6: Comparison of the Hα filaments (in red) with the distribution of blue light (in blue). The galactic continuum in the two images was removed by subtracting scaled green images.

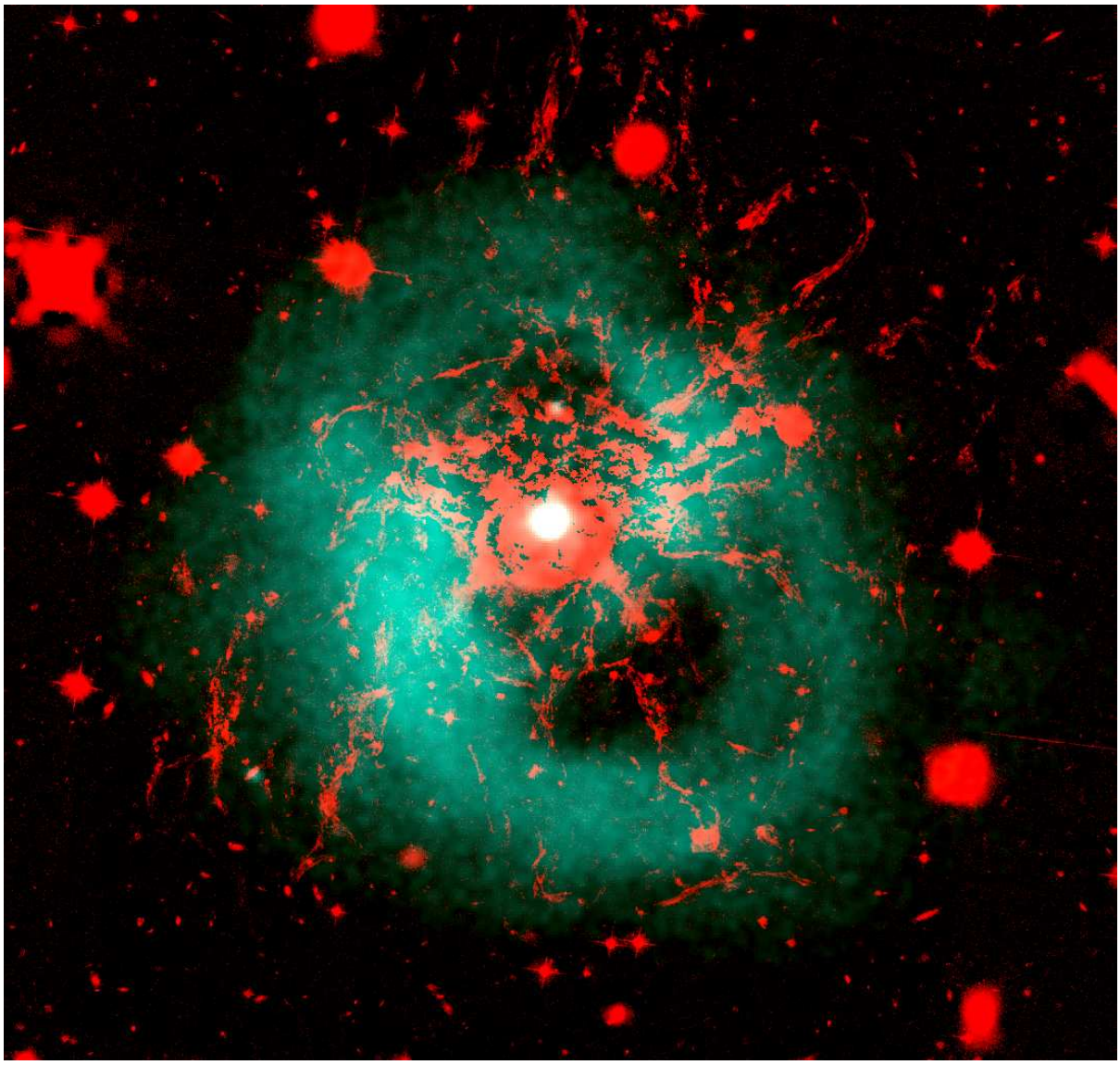

Figure 7: Comparison of the Hα filaments with the hard X-ray emission from the intracluster medium. The Hα image was formed from the red image, subtracting continuum and stellar-sources using SExtractor (as in Fig 2). The X-ray image is 900ks of Chandra data (Fabian et al 2006) in the 2 to 7 keV band, smoothed with a Gaussian with sigma=1.5 arcsec.

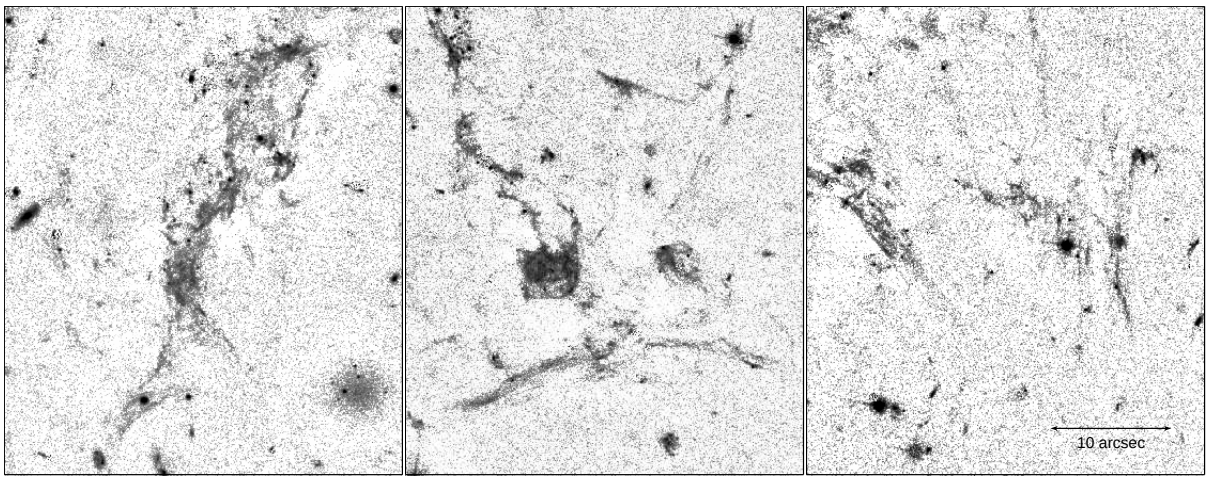

Figure 8: Detail of the 'Fish' and the S and W tangential filamentary regions. These are parts of the red image, showing the Hα filaments after subtracting the galactic continuum and stellar-sources using SExtractor (as in Fig 2).

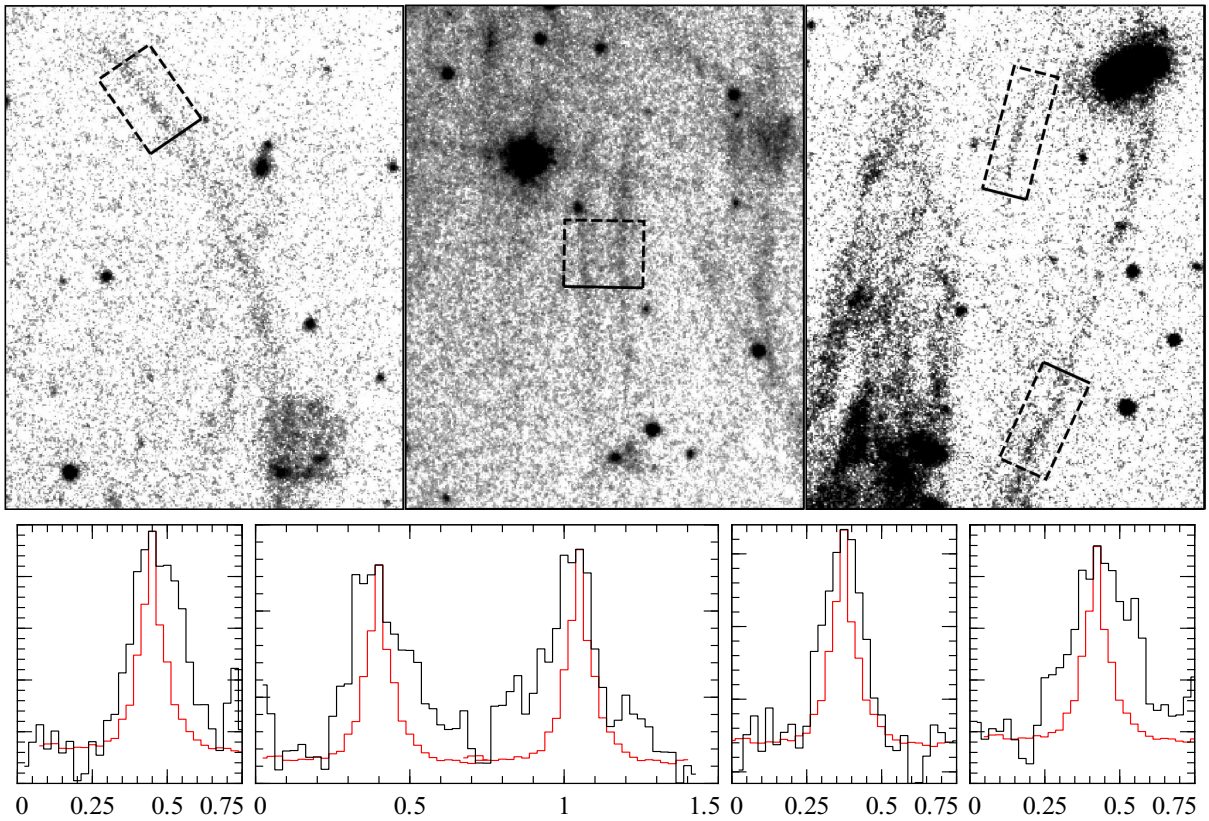

Figure 9: 1-D Hα flux profiles of the sections of the filaments marked by boxes in the three top panels. The solid axes of the boxes shows the direction of the profile, which were collapsed along the dotted axis. The bottom panels show the profiles extracted from the raw red image. The four leftmost bottom panels correspond to the four extraction regions shown. A typical stellar profile ($FWHM \sim 4$ pixels) is overlaid in red, which is less extended than any of the filament profiles (≥ 7 pixels). The x-axis is in units of one arcsec (pixels are 0.025 wide), the y-axis is intensity in arbitrary units.